Organic Electronics 11 (2010) 544–551

Contents lists available at ScienceDirect

Organic Electronics

journal homepage: www.elsevier.com/locate/orgel

Dibenzo[b,d]thiophene based oligomers with carbon–carbon unsaturated bonds for high performance field-effect transistors

Chengliang Wang [a,c], Zhongming Wei [a,c], Qing Meng [a,c], Huaping Zhao [a], Wei Xu [a], Hongxiang Li [b,*], Wenping Hu [a,*]

[a] Beijing National Laboratory for Molecular Sciences, Key Laboratory of Organic Solids, Institute of Chemistry, Chinese Academy of Sciences, Beijing 100190, PR China
[b] Laboratory of Material Science, Shanghai Institute of Organic Chemistry, Chinese Academy of Sciences, Shanghai 200032, PR China
[c] Graduate University of Chinese Academy of Sciences, Beijing 100039, PR China

ARTICLE INFO

Article history:
Received 30 October 2009
Received in revised form 18 December 2009
Accepted 18 December 2009
Available online 24 December 2009

Keywords:
Thin film transistors
Organic semiconductors
Oligomer

ABSTRACT

Dibenzo[b,d]thiophene (**DBT**) based oligomers with carbon–carbon double and triple bonds were synthesized. Their thermal stability and energy levels were studied by thermal analyses, UV–vis absorption spectra and electrochemistry. Single crystals of 3,7-bis(phenylethynyl)dibenzo[b,d]thiophene (**BEDBT**) revealed the introduction of unsaturated bonds eliminated the steric repulsion between adjacent aromatic rings and **BEDBT** displayed planar structure in crystals. Thin film transistors of these compounds displayed typical *p*-type behaviour. The best performance was obtained from 3,7-distyryldibenzo[b,d]thiophene (**DSDBT**) on OTS modified substrates with mobility as high as 0.15 cm^2/Vs and on/off current ratio up to 10^8, one of the highest performance for **DBT** based oligomers.

1. Introduction

Organic field-effect transistors (OFETs) have attracted great interest because of their merits (low cost, could be fabricated on large scale and on flexible substrates) and potential applications in flexible electronic devices (roll-up displays, smart card, RFID and so on) [1–4]. The typical structure of OFETs includes source, drain and gate electrodes, an organic semiconductor layer, and a dielectrical layer. Among them, organic semiconductor layer is the key point to determine the performance of OFETs. Till now, much progress has been made to the design and synthesis of novel organic semiconductors for OFETs. Some organic semiconductors such as pentacene and heteroacenes with mobility larger than 0.5 cm^2/Vs have been reported [5–11]. The reason for the high performance of these fused ring organic semiconductors could be attributed to their large planar conjugated structures which would lead to large charge transfer integral and low reorganization energy. However, these fused ring compounds usually suffered tedious synthesis steps, complex purifications, low stabilities and solubilities. Studies have showed that oligomers would have good solubility and are easy to be modified to fit different applications, but oligomers usually exhibit low device performance because of their non-planar structures caused by the steric repulsion between adjacent aromatic rings [12–17]. We and some researchers have reported, by introduction of carbon–carbon double [18–24] and triple bonds [25–32], planar conjugated oligomers which combined the merits of fused ring compounds and single bonds linked oligomers can be obtained. For instance, phenylvinylene oligomer [19] and its alkyl functionalized derivates [20] showed a maximum mobility of 1.3 cm^2/Vs; similar thiophenylvinylene oligomers [21] exhibited mobility up to 0.4 cm^2/Vs, seven times of its single bonds linked components [13,14]. Similar results have also been observed from the organic semiconductors with carbon–carbon triple bonds. For example, single crystals of 9,10-bisphenylethynyleneanthracene showed mobility as high as 0.73 cm^2/Vs [26]; the performances of transistors

* Corresponding authors.
E-mail addresses: lhx@mail.sioc.ac.cn (H. Li), huwp@iccas.ac.cn (W. Hu).

1566-1199/$ - see front matter © 2009 Elsevier B.V. All rights reserved.
doi:10.1016/j.orgel.2009.12.011

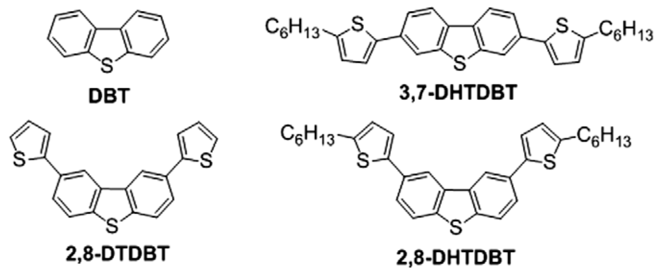

Scheme 1. The chemical structures of **DBT** and some of its single bonds linked oligomers.

of thiophene-phenyl cooligomers with carbon–carbon triple bonds was much better than those of their single bond components [25].

Dibenzo[b,d]thiophene (**DBT**, chemical structure see Scheme 1) is a commercial available chalcogenophene coumpound [33,34]. It has high ionization potential compared with anthracene, fluorene and carbazole which has conjugated planar structure and is commonly used as blocking unit in semiconductors. Additionally, the S atoms in **DBT** could introduce S···S and S···π intermolecular interactions which might facilitate charge transport. All of these merits suggested that **DBT** should be an ideal conjugated unit for organic semiconductors. In our previous work [34], we have observed single bonds linked **DBT** oligomer 3,7-bis(5′-hexylthiophene-2′-yl)dibenzothiophene (**3,7-DHTDBT**) displayed good transistor performance. In order to further investigate the application of **DBT** in organic semiconductors and the effect of carbon–carbon double and triple bonds to the performance of materials, herein two new 3,7-disubstituted **DBT** derivates, 3,7-bis(phenylethynyl)dibenzo[b,d]thiophene (**BEDBT**) and 3,7-distyryldibenzo[b,d]thiophene (**DSDBT**) were synthesized. Their physicochemical properties and charge transport characteristics were studied.

2. Results and discussion

The synthesis routes of **BEDBT** and **DSDBT** were outlined in Scheme 2. **BEDBT** were synthesized through modified Pd catalyzed Sonogashira coupling reaction [35]. **DSDBT** were synthesized through Heck reaction using $Pd(OAc)_2$ as catalyst [36]. **BEDBT** was easy to form crystals and was purified through recrystallization from toluene. **DSDBT** was obtained through column chromatography and further purified by vacuum sublimation. Both compounds were soluble in normal organic solvents such as CH_2Cl_2, THF, toluene and chlorobenzene, and totally characterized by ^1H NMR, MS and elementary analysis.

Single crystals of **BEDBT** suitable for X-ray diffraction (XRD) measurements were grown from toluene solution. As we expected, the single crystals of **BEDBT** revealed that it had nearly planar structure and belonged to a crystal system of monoclinic space group $P2_1$ with unit-cell parameters of $a = 11.666(2)$, $b = 7.6007(15)$, $c = 22.162(4)$ Å and $\beta = 94.89(3)°$. As showed in Fig. 1A, **BEDBT** adopted herringbone geometry in the crystals, and the herringbone angle was about 51.7°. Interestingly, adjacent **BEDBT** molecules along a axis formed Head-to-Head and Tail-to-Tail pairs (relative to S atoms). Fig. 1B showed the intermolecular interactions among neighbor molecules along a axis. S···H, S···π and C–H···π intermolecular interactions were found in Head-to-Head pairs, and only C–H···π intermolecular interactions existed in Tail-to-Tail pairs.

The thermal stabilities of **BEDBT** and **DSDBT** were characterized by thermogravimetric analysis (TGA). From their TGA curves (see Supplementary data), we could see **BEDBT** and **DSDBT** decomposed onset of 300 °C and 350 °C respectively, suggesting their good thermal stabilities. Fig. 2A showed the UV–vis absorption spectra of **BEDBT** and **DSDBT** in CH_2Cl_2 solution at the concentration of 10^{-5} M. The two compounds showed similar absorption peaks, but the maximum absorption of **DSDBT** was about 30 nm red shift than that of **BEDBT**, indicating a larger π-conjugation length of **DSDBT**. This phenomenon has also been observed by others [25,37]. The optical energy gaps estimated from UV–vis spectra were 3.35 and 3.1 eV for **BEDBT** and **DSDBT** respectively. The UV–vis absorption of vacuum deposited thin films of **BEDBT** and **DSDBT** were also tested to show the molecular arrangement in solids. They all showed very broad absorptions and the initial absorptions were red shifted compared with those of the solutions, indicating the ordered arrangements in solid states. The cyclic voltammetry of **BEDBT** and **DSDBT** in CH_2Cl_2 solutions at the concentration of 10^{-3} M were illustrated in Fig. 2B and C (using ferrocene (Cp_2Fe) as internal standard substance). The HOMO energy levels calculated from electrochemistry were −5.87 eV for **BEDBT** and −5.57 eV for **DSDBT** (the HOMO energy level of ferrocene was about −4.8 eV). The HOMO energy level of **BEDBT** was even lower than 2,8-disubstituted **DBT** derivatives 2,8-di(5’-hexyl-thiophen-2’-yl)-dibenzothiophene (**2,8-DHTDBT**, chemical structure see Scheme 1) reported in our previous work [33]. The lower HOMO energy level of **BEDBT** should be attributed to its short conjugated length (which was determined by UV–vis spectrum), the high ionic potential of **DBT** and the stronger electron-withdrawing effect of ethynylene group than that of the vinyl group. And this low HOMO energy level would cause carriers accumulation difficulty and charge injection barrier, which usually leads to low transistor performance. The energy gaps and HOMO/LUMO energy levels of **BEDBT** and **DSDBT** were summarized in Fig. 2D. The low HOMO energy levels suggested the good environmental stability of **BEDBT** and **DSDBT**.

The charge transport properties of **BEDBT** and **DSDBT** were examined to study their applications in OFETs. The

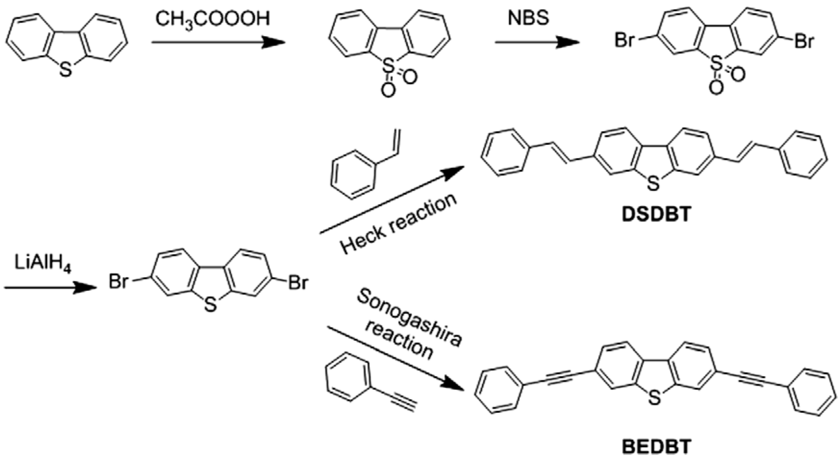

Scheme 2. Synthesis routes of **DSDBT** and **BEDBT**.

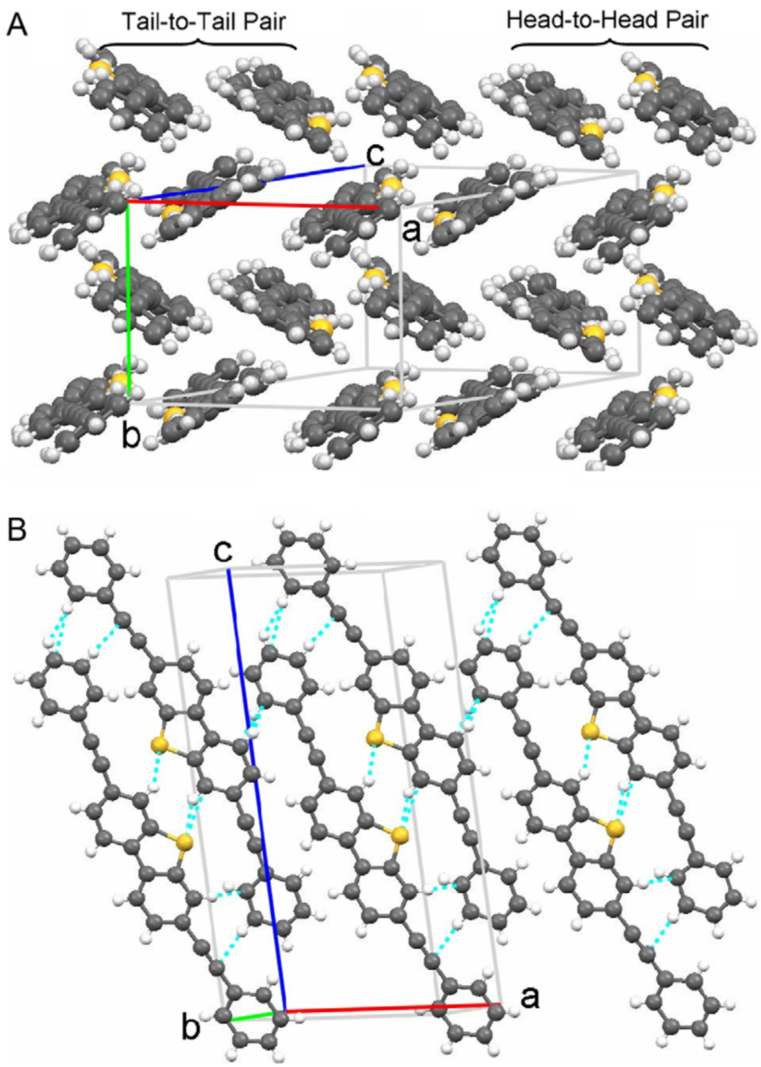

Fig. 1. (A) Packing diagram of **BEDBT**, (B) intermolecular interactions between Head-to-Head and Tail-to-Tail pairs along *a* axis in **BEDBT** crystals.

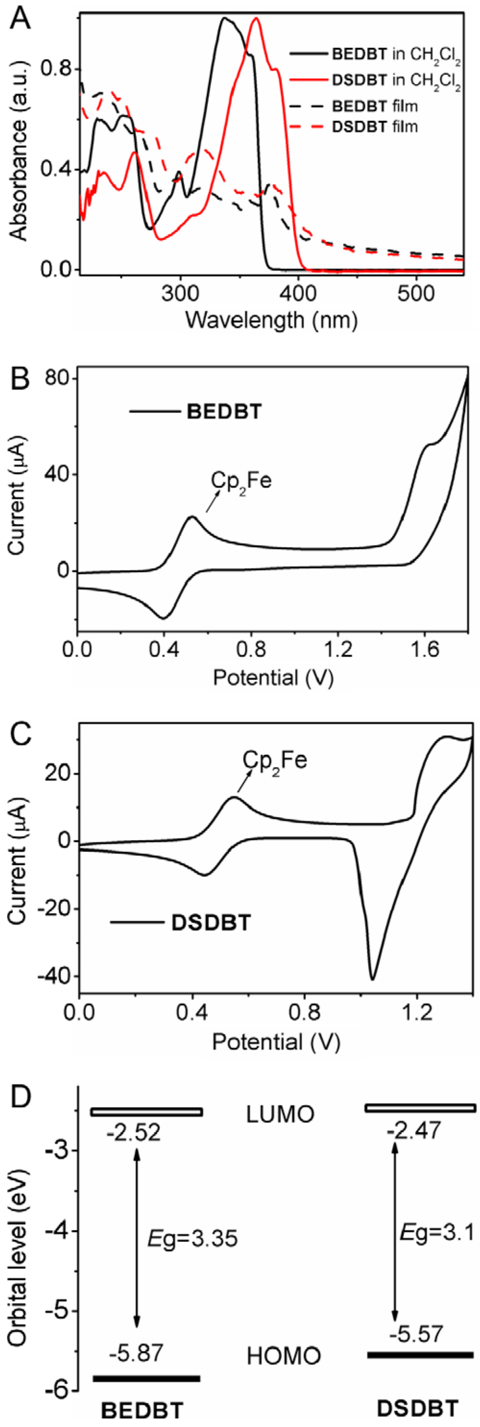

Fig. 2. (A) UV–vis absorption spectra, (B and C) cyclic voltammograms and (D) orbital levels of **BEDBT** and **DSDBT**.

transistors were fabricated in top-contact mode using gold as the source and drain electrodes. The field-effect mobilities (μ) were calculated in the saturation regime according to the following equation: $I_D = \mu Ci(W/2L)(V_G - V_T)^2$, where I_D is the drain current, Ci is the capacitance per unit area of the gate dielectric, W and L are the channel width and length, respectively, V_G and V_T are the gate and threshold voltage, respectively. All the devices showed typical *p*-type channel FET performance under ambient conditions. Fig. 3 showed typical transfer and output curves of an example device obtained at 50 °C on octadecyltrichlorosilane (OTS) modified SiO_2/Si substrates using **DSDBT** as a semiconductor layer. The FET performance of **DSDBT** and **BEDBT** on different deposition temperature were summarized in Table 1. From Table 1, we could see the devices of **DSDBT** displayed mobility larger than 0.03 cm^2/Vs. And when the temperature of substrate increased (from 25 °C to 50 °C), the mobility of devices increased; further increasing the substrate temperature, the performance of devices decreased. The highest mobility of **DSDBT** could reach up to 0.15 cm^2/Vs, one of the highest mobility reported for **DBT** based oligomers. While scanning V_G from 0 to −120 V and then retraced scanning from −120 to 0 V at $V_{DS} = -100$ V, hysteresis behaviour was observed (Fig. 3A). This might be attributed to the instability of the oxidized species which was proved by the irreversible oxidations from the electrochemistry results. The performance of **BEDBT** devices was much lower compared with **DSDBT**, which was probably due to its lower HOMO energy level. The highest performance of **BEDBT** devices was obtained at $T_{sub} = 25$ °C.

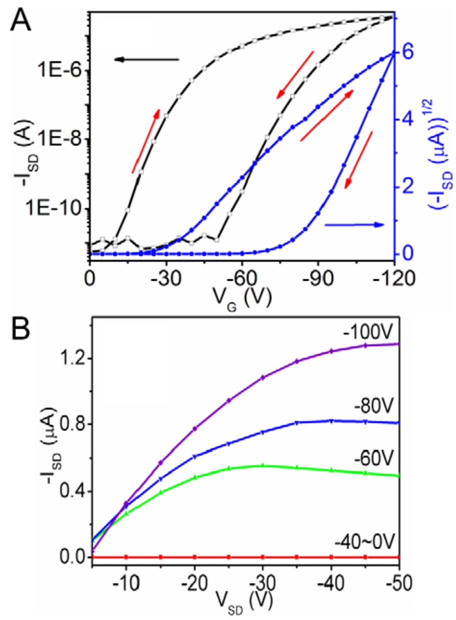

Fig. 3. (A) An example transfer with hysteresis loop ($V_{DS} = -100$ V) and (B) output curves of devices based on **DSDBT** films deposited on OTS modified SiO_2/Si substrates at 50 °C.

In order to investigate the mobility-substrate temperature dependence, the morphologies and the structures of **DSDBT** and **BEDBT** films deposited at different substrate temperature were investigated by atomic force microscopy (Fig. 4 for **DSDBT** and Fig. 5 for **BEDBT**) and X-ray diffraction (Fig. 6) respectively. From the AFM images, we could see with the increase of substrate temperature, the grain size of **DSDBT** film increased. The step height of crystalline terrace layers at $T_{sub} = 50$ °C was about 2.2 nm (Fig. 4E, left)

Table 1
FET characteristics of **DSDBT** and **BEDBT** prepared by vacuum deposition on OTS modified SiO_2/Si substrates at different temperatures.

Entry	T_{sub} (°C)	μ_{max} (cm^2/Vs)	On/off ratio
DSDBT	25	0.039	4×10^6
	50	0.15	2×10^8
	100	0.06	3×10^7
BEDBT	25	1.3×10^{-4}	7×10^5
	50	8.0×10^{-5}	9×10^4

which was nearly equal to the simulated molecular length (about 2.24 nm) by minimized energy optimization (Fig. 4E, right), indicating that the **DSDBT** molecules grown layer-by-layer and took nearly perpendicular orientation on the substrate in the films. Further increasing the substrate temperature to 100 °C, larger grain was obtained. However, the continuity of the films became worse (see Supplementary data), and this should take the responsibility for the lower device performance at T_{sub} = 100 °C. From

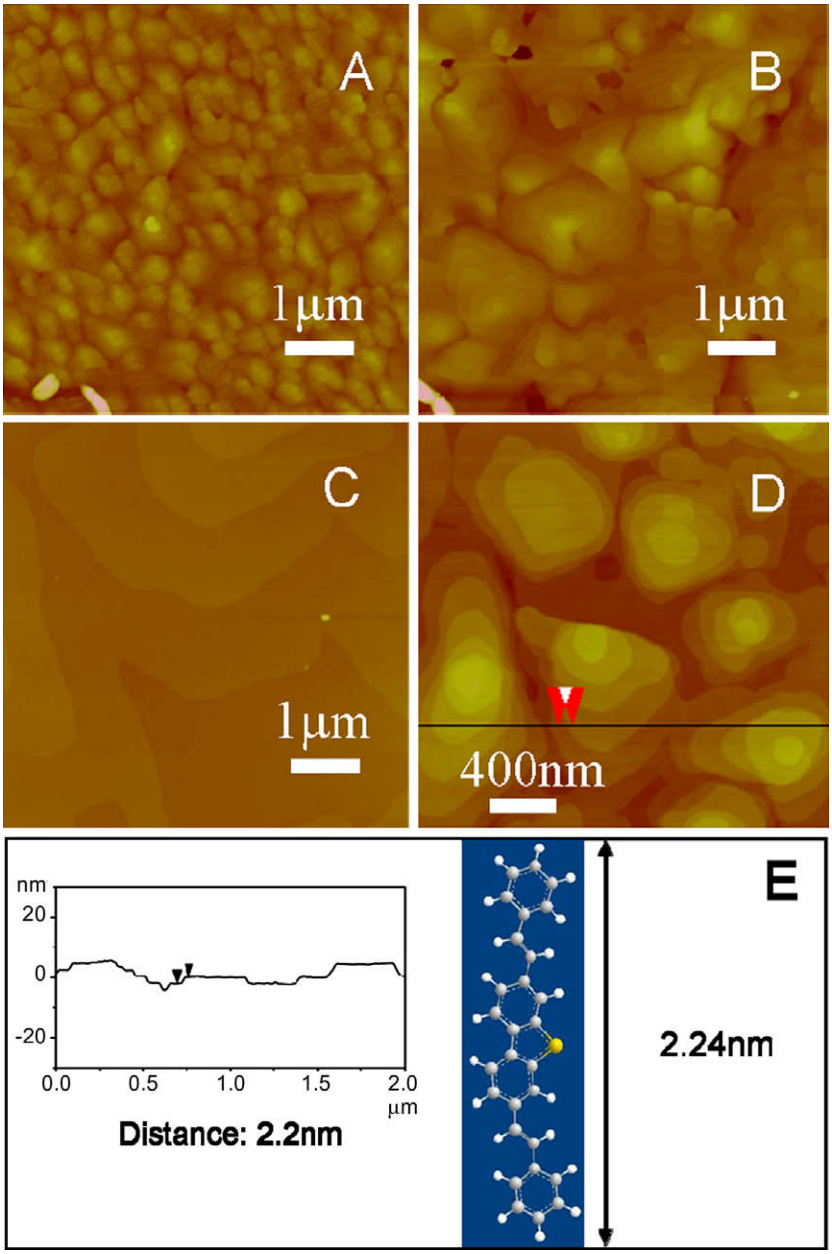

Fig. 4. (A–C) AFM images (5 × 5 μm) of thin films of **DSDBT** on OTS modified SiO_2/Si substrates at the substrate temperature of (A) 25 °C, (B) 50 °C, (C) 100 °C. (D) AFM images (2 × 2 μm) of **DSDBT** thin films on OTS modified SiO_2/Si substrate at the substrate temperature of 50 °C and (E) the step heights of crystalline terrace layers as measured by a section analysis along the line marked in (D) (left) and optimized model molecular structure (right).

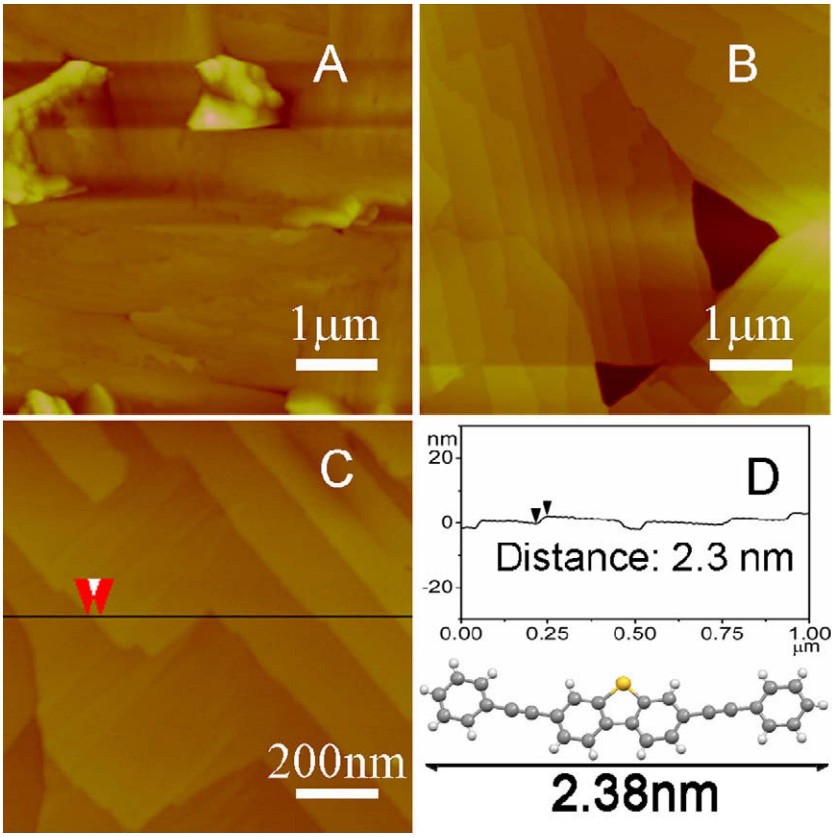

Fig. 5. (A and B) AFM images (5 × 5 μm) of **BEDBT** thin films on OTS modified SiO_2/Si substrates at the substrate temperature of (A) 25 °C, (B) 50 °C. (C) AFM images (1 × 1 μm) of **BEDBT** thin films on OTS modified SiO_2/Si substrates at the substrate temperature of 25 °C and (D) the step heights of crystalline terrace layers as measured by a section analysis along the line marked in (C) (top) and molecular structure in crystal (bottom).

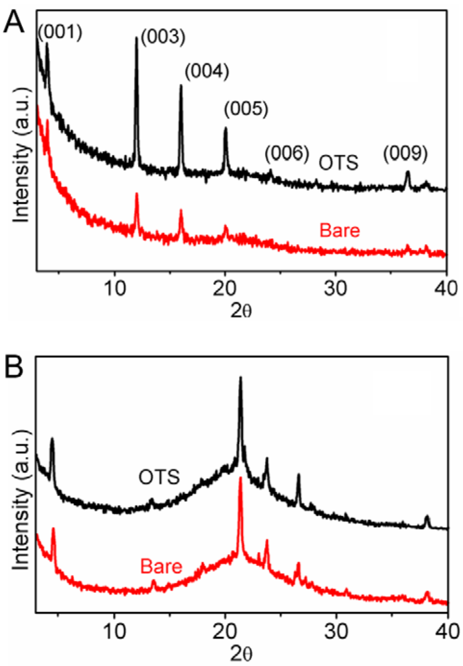

Fig. 6. XRD patterns of thin films of (A) **DSDBT** and (B) **BEDBT** on bare and OTS modified SiO_2/Si substrate at 25 °C.

the XRD patterns of **DSDBT** films (Fig. 6B), the *d*-spacing determined from their dominant peaks were 1.97 nm, closed to the simulated molecular length (2.24 nm), which also proved that the molecules were grown almost vertically to the substrates when deposited. **BEDBT** films exhibited similar results as **DSDBT**. When the substrate temperature increased to 50 °C, larger grains were obtained, but larger grain boundaries were also formed at the same time. The step height of layers of thin films determined from AFM results was about 2.3 nm (very close to the molecular length, Fig. 5D), suggesting **BEDBT** was grown layer-by-layer and nearly vertically on the substrate.

3. Conclusions

In summary, dibenzothiophene oligomers with carbon–carbon double and triple bonds were synthesized. TGA, UV–vis spectra and electrochemistry results indicated that both compounds had high stability and high oxidation resistance. Single crystal structure of **BEDBT** revealed that the introduction of carbon–carbon unsaturated bonds eliminated the steric repulsions between adjacent aromatic rings. Thin film transistors of these compounds exhibited typical *p*-channel performance. **DSDBT** displayed high FET performance with mobility up to 0.15 cm^2/Vs, and on/off ratio as high as 10^8. The performance of **BEDBT** was much lower compared with **DSDBT**, which could be attributed to its smaller π-conjugated system and lower HOMO energy level. Further optimization of the devices, field-effect transistors based on solution-processed films and single crystals of these materials are underway.

4. Experimental

4.1. General

All reactants and solvents were purchased from commercial suppliers and used as received unless ultra noted. The reactant 3,7-dibromodibenzo[b,d]thiophene was synthesized using *N*-bromosuccinimide (NBS) as bromination reagent according to literature [34,38–39]. MS (EI) was recorded on a Shimadzu GCMS-QP2010 Plus mass spectrometer. ^{1}H NMR spectra were obtained on a Varian 400 MHz spectrometer in $CDCl_3$ with tetramethylsilane as an internal reference. Elemental analyses were performed on a Carlo Erba model 1160 elemental analyzer. UV–vis spectra were recorded on a Hitachi U-3010 spectrometer. Cyclic voltammograms were obtained on a CHI660C analyzer in a conventional three-electrode cell using a glassy carbon working electrode, a platinum wire counter electrode, an Ag/AgCl reference electrode and Bu_4NPF_6 as supporting electrolyte. X-ray diffraction (XRD) measurements for films were carried out on a *D*/max2500 instrument (Cu Kα radiation, λ = 1.54056 Å). XRD measurements for single crystals were carried out in the reflection mode using a Rigaku Saturn CCD area detector system (Mo Kα radiation, λ = 0.71073 Å). AFM images were obtained in air using a Digital Instruments Nanoscope III in tapping mode.

4.2. Materials synthesis

4.2.1. Synthesis of 3,7-distyryldibenzo[b,d]thiophene (*DSDBT*)

A 100 mL flask was charged with 3,7-dibromodibenzo-[b,d]thiophene (1.71 g, 5 mmol), PPh_3 (0.13 g, 0.5 mmol), $Pd(OAc)_2$ (0.112 g, 0.5 mmol) and dry Et_3N (20 mL). After the mixture was degassed three times and backfilled with N_2, styrene (5.2 g, 50 mmol) was added. The reaction solution was stirred at 100 °C for 3 days. The mixture was evaporated under reduced pressure. The residual solid was purified by chromatography on silica gel (petroleum ether:dichloromethane = 1:1) to provide **DSDBT** as light yellow powder (yield: 1.2 g, 62%). mp: >300 °C. MS (EI) *m*/*z*: 388 [M$^+$]. ^{1}H NMR (400 MHz, $CDCl_3$): 8.01 (d, 2H), 7.97 (s, 2H), 7.64 (d, 2H), 7.56 (d, 4H), 7.39 (t, 4H), 7.29 (t, 2H), 7.24 (d, 4H). Anal. calcd for $C_{28}H_{20}S$: C, 86.56; H, 5.19; found: C, 86.31; H, 5.28.

4.2.2. Synthesis of 3,7-bis(phenylethynyl)dibenzo[b,d]-thiophene (*BEDBT*)

A 100 mL flask was charged with 3,7-dibromodibenzo[b,d]thiophene (1.71 g, 5 mmol), $Pd(PPh_3)_2Cl_2$ (0.21 g, 0.3 mmol), CuI (0.115 g, 0.6 mmol), THF (30 mL) and aqueous 2-aminoethanol (2 M, 20 mL). After the mixture was degassed three times and backfilled with N_2, phenylacetylene (1.86 g, 18 mmol) was added. The reaction solution was stirred at 80 °C overnight. THF was removed, and the aqueous layer was extracted by CH_2Cl_2. The combined organic layer was evaporated under reduced pressure. The residual solid was purified by recrystallization from toluene to give **BEDBT** as white crystals (yield: 1.15 g, 60%). mp: 234 °C. MS (EI) *m*/*z*: 384 [M$^+$]. ^{1}H NMR (400 MHz, $CDCl_3$): 8.10 (d, 2H), 8.03 (s, 2H), 7.63 (d, 2H), 7.57 (m, 4H), 7.37 (m, 6H). Anal. calcd for $C_{28}H_{16}S$: C, 87.47; H, 4.19; found: C, 87.25; H, 4.29.

4.3. Device fabrication and electrical characterization

The SiO_2/Si substrates used were heavily doped *n*-type Si wafer with 500 nm-thick SiO_2 layer and capacitance of 7.5 nF/cm^2. After rinsed with conc. H_2SO_4/H_2O_2, water, and iso-propanol, they were surface modified with OTS. Before sublimation, the OTS modified substrates were rinsed with hexane, chloroform and iso-propanol successively. The organic semiconductors were deposited at a rate increasing gradually under a pressure of about 10^{-4} Pa to a final thickness of 50 nm determined by a quartz crystal monitor. The source and drain electrodes were deposited with gold by using shadow masks with W/L of ca. 48.2. Device characteristics were obtained with a Keithley 4200 SCS and Micromanipulator 6150 probe station in a clean and shielded box at room temperature in air.

Acknowledgements

This work was supported by National Natural Science Foundation of China (60771031, 60736004, 20571079, 20721061 and 50725311), Ministry of Science and Technology of China (2006CB806200, 2006CB932100) and Chinese Academy of Sciences.

Appendix A. Supplementary data

Supplementary data associated with this article can be found, in the online version, at doi:10.1016/j.orgel.2009.12.011.

References

[1] S.R. Forrest, Chem. Rev. 97 (1997) 1793.
[2] J. Zaumseil, H. Sirringhaus, Chem. Rev. 107 (2007) 1296.
[3] V. Coropceanu, J. Cornil, D.A. da Silva Filho, Y. Olivier, R. Silbey, J.-L. Brédas, Chem. Rev. 107 (2007) 926.
[4] A.J. Baca, J.-H. Ahn, Y. Sun, M.A. Meitl, E. Menard, H.-S. Kim, W.M. Choi, D.-H. Kim, Y. Huang, J.A. Rogers, Angew. Chem. Int. Ed. 47 (2008) 5524.
[5] Y.Y. Lin, D.J. Gundlach, S.F. Nelson, T.N. Jackson, IEEE Electron Device Lett. 18 (1997) 606.
[6] K. Xiao, Y. Liu, T. Qi, W. Zhang, F. Wang, J. Gao, W. Qiu, Y. Ma, G. Cui, S. Chen, X. Zhan, G. Yu, J. Qin, W. Hu, D. Zhu, J. Am. Chem. Soc. 127 (2005) 13281.
[7] M.L. Tang, S.C.B. Mannsfeld, Y.-S. Sun, H.A. Becerril, Z. Bao, J. Am. Chem. Soc. 131 (2009) 882.
[8] M.L. Tang, T. Okamoto, Z. Bao, J. Am. Chem. Soc. 128 (2006) 16002.
[9] K. Takimiya, H. Ebata, K. Sakamoto, T. Izawa, T. Otsubo, Y. Kunugi, J. Am. Chem. Soc. 128 (2006) 12604.
[10] T. Yamamoto, K. Takimiya, J. Am. Chem. Soc. 129 (2007) 2224.
[11] T. Okamoto, K. Kudoh, A. Wakamiya, S. Yamaguchi, Org. Lett. 7 (2005) 5301.
[12] M.L. Tang, M.E. Roberts, J.J. Locklin, M.M. Ling, H. Meng, Z. Bao, Chem. Mater. 18 (2006) 6250.

[13] H. Meng, F. Sun, M.B. Goldfinger, G.D. Jaycox, Z. Li, W.J. Marshall, G.S. Blackman, J. Am. Chem. Soc. 127 (2005) 2406.
[14] S. Ando, J.-I. Nishida, E. Fujiwara, H. Tada, Y. Inoue, S. Tokito, Y. Yamashita, Chem. Mater. 17 (2005) 1261.
[15] H. Meng, J. Zheng, A.J. Lovinger, B. Wang, P.G. Van Patten, Z. Bao, Chem. Mater. 15 (2003) 1778.
[16] K. Ito, T. Suzuki, Y. Sakamoto, D. Kubota, Y. Inoue, F. Sato, S. Tokito, Angew. Chem. Int. Ed. 42 (2003) 1159.
[17] D. Kumaki, T. Umeda, T. Suzuki, S. Tokito, Org. Electron. 9 (2008) 921.
[18] C. Videlot-Ackermann, J. Ackermann, H. Brisset, K. Kawamura, N. Yoshimoto, P. Raynal, A.E. Kassmi, F. Fages, J. Am. Chem. Soc. 127 (2005) 16346.
[19] H. Klauk, U. Zschieschang, R.T. Weitz, H. Meng, F. Sun, G. Nunes, D.E. Keys, C.R. Fincher, Z. Xiang, Adv. Mater. 19 (2007) 3882.
[20] H. Meng, F. Sun, M.B. Goldfinger, F. Gao, D.J. Londono, W.J. Marshal, G.S. Blackman, K.D. Dobbs, D.E. Keys, J. Am. Chem. Soc. 128 (2006) 9304.
[21] M.C. Um, J. Jang, J. Kang, J.P. Hong, D.Y. Yoon, S.H. Lee, J.J. Kim, J.I. Hong, J. Mater. Chem. 18 (2008) 2234.
[22] N. Drolet, J.-F. Morin, N. Leclerc, S. Wakim, Y. Tao, M. Leclerc, Adv. Funct. Mater. 15 (2005) 1671.
[23] L. Zhang, L. Tan, Z. Wang, W. Hu, D. Zhu, Chem. Mater. 21 (2009) 1993.
[24] J. Ronacali, Acc. Chem. Res. 33 (2000) 147.
[25] Q. Meng, J. Gao, R. Li, L. Jiang, C. Wang, H. Zhao, C. Liu, H. Li, W. Hu, J. Mater. Chem. 19 (2009) 1477.
[26] C. Wang, Y. Liu, Z. Ji, E. Wang, R. Li, H. Jiang, Q. Tang, H. Li, W. Hu, Chem. Mater. 21 (2009) 2840.
[27] W. Cui, X. Zhang, X. Jiang, H. Tian, D. Yan, Y. Geng, X. Jing, F. Wang, Org. Lett. 8 (2006) 785.
[28] V.A.L. Roy, Y.-G. Zhi, Z.-X. Xu, S.-C. Yu, P.W.H. Chan, C.-M. Che, Adv. Mater. 17 (2005) 1258.
[29] W. Zhao, Q. Tang, H.S. Chan, J. Xu, K.Y. Lo, Q. Miao, Chem. Commun. (2008) 4324.
[30] A. Marrocchi, M. Seri, C. Kim, A. Facchetti, A. Taticchi, T.J. Marks, Chem. Mater. 21 (2009) 2592.
[31] N.S. Baek, S.K. Hau, H.-L. Yip, O. Acton, K.-S. Chen, A.K.-Y. Jen, Chem. Mater. 20 (2008) 5734.
[32] C.P. Gerlach, T.W. Kelley, D.V. Muyres, New, High-Performance Acenyl Semiconductors, in: 227th ACS National Meeting, Anaheim, CA, 2004.
[33] B. Chawla, F.D. Sanzo, J. Chromatogr. 589 (1992) 271.
[34] J. Gao, L. Li, Q. Meng, R. Li, H. Jiang, H. Li, W. Hu, J. Mater. Chem. 17 (2007) 1421.
[35] M.S.M. Ahmed, A. Mori, Tetrahedron 60 (2004) 9977.
[36] H. Kang, G. Evmenenko, P. Dutta, K. Clays, K. Song, T.J. Marks, J. Am. Chem. Soc. 128 (2006) 6194.
[37] C. Videlot-Ackermann, J. Ackermann, K. Kawamura, N. Yoshimoto, H. Brisset, P. Raynal, A. El Kassmi, F. Fages, Org. Elecron. 7 (2006) 465.
[38] H. Sirringhaus, R.H. Friend, C. Wang, J. Leuninger, K. Müllen, J. Mater. Chem. 9 (1999) 2095.
[39] I.I. Perepichka, I.F. Perepichka, M.R. bryce, L.-O. Pålsson, Chem. Commun. (2005) 3397.